Hindawi
Advances in Civil Engineering
Volume 2019, Article ID 4098505, 18 pages
https://doi.org/10.1155/2019/4098505

Research Article

Using Steel Fiber-Reinforced Concrete Precast Panels for Strengthening in Shear of Beams: An Experimental and Analytical Investigation

Pitcha Jongvivatsakul,[1] **Linh V. H. Bui**,[1,2] **Theethawachr Koyekaewphring**,[3] **Atichon Kunawisarut**,[4] **Narawit Hemstapat**,[4] **and Boonchai Stitmannaithum**[1]

[1]*Innovative Construction Materials Research Unit, Department of Civil Engineering, Faculty of Engineering, Chulalongkorn University, 254 Phayathai Road, Pathumwan, Bangkok 10330, Thailand*
[2]*Department of Civil Engineering, Industrial University of Ho Chi Minh City, 12 Nguyen Van Bao, Ward 4, Go Vap District, Ho Chi Minh City 700000, Vietnam*
[3]*Department of Civil Engineering, Faculty of Engineering, Chulalongkorn University, 254 Phayathai Road, Pathumwan, Bangkok 10330, Thailand*
[4]*Department of Civil and Environmental Engineering, Tokyo Institute of Technology, 2-12-1-M1-21 Ookayama, Meguro-ku, Tokyo 152-8552, Japan*

Correspondence should be addressed to Pitcha Jongvivatsakul; pitcha.j@chula.ac.th

Received 14 February 2019; Revised 5 April 2019; Accepted 17 April 2019; Published 2 June 2019

Academic Editor: Flora Faleschini

In this paper, the performances of reinforced concrete (RC) beams strengthened in shear with steel fiber-reinforced concrete (SFRC) panels are investigated through experiment, analytical computation, and numerical analysis. An experimental program of RC beams strengthened by using SFRC panels, which were attached to both sides of the beams, is carried out to investigate the effects of fiber volume fraction, connection type, and number and diameter of bolts on the structural responses of the retrofitted beams. The current shear resisting model is also employed to discuss the test data considering shear contribution of SFRC panels. The experimental results indicate that the shear effectiveness of the beams strengthened by using SFRC panels is significantly improved. A three-dimensional (3D) nonlinear finite element (FE) analysis adopting ABAQUS is also conducted to simulate the beams strengthened in shear with SFRC panels. The investigation reveals the good agreement between the experimental and analytical results in terms of the mechanical behaviors. To complement the analytical study, a parametric study is performed to further evaluate the influences of panel thickness, compressive strength of SFRC, and bolt pattern on the performances of the beams. Based on the numerical and experimental analysis, a shear resisting model incorporating the simple formulation of average tensile strength perpendicular to the diagonal crack of the strengthened SFRC panels is proposed with the acceptable accuracy for predicting the shear contribution of the SFRC system under various effects.

1. Introduction

Deterioration of reinforced concrete (RC) structures is increasing nowadays due to the degradation of structural materials, the increase in design load, and the damage arising from disasters such as earthquake and fire. One common strengthening technique for RC members is the use of fiber-reinforced polymer (FRP) composites, which aims to resist the tensile forces in the needed regions. Many researchers have investigated the performance of concrete beams strengthened by FRP composites under flexure, shear, and fatigue conditions [1–13]. Their studies indicated the effectiveness of the beams strengthened by FRP composites in terms of the capacity enhancement, ductility, and corrosion prevention improvement. It was also shown in the past studies that the strengthening FRP system could restore the

members' strength. Nevertheless, the FRP strengthening system can be debonded before reaching their rupture strength, which can cause brittle behavior [14–18], showing the under capability of the FRP composites.

On the contrary, strengthening by fiber-reinforced concrete (FRC) is one technique of interest since the addition of short discrete fibers to concrete could improve tensile strength, toughness, and ductility as discussed in the researches [19–24]. The findings in those studies showed the significant improvement in mechanical properties of concrete containing steel fibers. Recently, as presented in the studies [25, 26], the uses of fiber-reinforced concrete and fiber-reinforced cement composites as strengthening and repairing materials could exhibit the enhancement in the load-displacement performances due to the effectiveness of steel fibers. Additionally, Martinola et al. [27] and Kobayashi and Rokugo [28] used high-performance fiber-reinforced concrete (HPFRC) to strengthen RC beams by jacketing and patching, respectively. The results showed that the proposed technique provided the structural improvement both at ultimate and serviceability limit states. In addition, due to the impressive properties, the steel-reinforced strain-hardening cementitious composites (SHCCs) were utilized for the strengthening of RC beams as reported by Hussein et al. [29]. This work confirmed that the strengthening by using SHCCs can enhance ductility of RC beams. Besides, the intervention technique utilizing the combination of high-performance fiber-reinforced cement-based composite (HPFRCC) and carbon fiber-reinforced polymer (CFRP) was discussed by Ferrari et al. [30]. It is found that a better transition layer for CFRP sheets is achieved when HPFRCC is used. However, these studies focused mainly on the flexural behavior of the retrofitted members. There are some publications relating to the shear strengthening of RC beams using fiber-reinforced concrete [31–37]. Wirojjanapirom et al. [31] introduced the use of ultra high strength fiber-reinforced concrete permanent formwork for enhancing the shear capacity of RC beams. Ruano et al. [32] used the cast-in-place FRC jacketing with different fiber dosages to improve shear capacity of the RC beams. Other materials such as textile-reinforced mortar (TRMs) [33, 34], cement-based fiber composite material [35, 36], and self-compacting concrete jacketing [37] were also studied to extend the understanding on the shear performances of the members strengthened by FRC composites. However, on the basis of a careful literature search, the research on shear strengthening using steel fiber-reinforced concrete (SFRC) is relatively limited not only in the experimental field but also in the analytical field, especially the use of SFRC precast panels for retrofitting the current structures has not shown in the past studies.

In this study, the new shear strengthening method for the RC beams is introduced. The steel fiber-reinforced concrete (SFRC) panels were attached to the shear zones through adhesive and bolts. These SFRC panels are precast members which can be prepared in advance and easily installed at site. In order to verify the effectiveness of this intervention technique, the experimental tests, finite element analysis, and analytical model of the RC beams strengthened by using SFRC panels are carried out as follows: (1) the structural responses of RC beams after strengthening is investigated to show the strengthening efficiency of the SFRC panels. (2) The applicability of the current shear resisting model proposed by JSCE 2006 [38] for calculating the shear contribution of SFRC strengthening system is also presented. In addition, (3) the experimental and analytical results are compared to validate the finite element (FE) tool in simulating the beams strengthened by using SFRC panels. Then, (4) the parametric study is extended by means of FE analysis to include optimum parameters for investigating the performances of the RC beams strengthened in shear by SFRC precast panels under various influences which are necessary for the practical use. Moreover, (5) based on the obtained numerical and experimental analyses, a simple model for predicting the shear resisting force of the retrofitted SFRC panels connected to the beams' sides using adhesive resin and bolts is proposed with considerable accuracy.

2. Experimental Program

2.1. Investigation Factors. The experimental program consisted of nine rectangular RC beams. The parameters investigated were (1) steel fiber volume fraction, (2) connection types, (3) number of bolts, and (4) diameter of bolt. Table 1 summarizes the experimental cases. There was one control beam without strengthening. Eight beams were strengthened using four panels on each side of the beams at shear span. The steel fiber volume fractions of the strengthening panels were 0, 1.0, and 1.5%. The connection types between RC beams and panels were epoxy and bolts with epoxy. The number of bolts used per panel varied with the amount of 4, 6, and 8 bolts. The diameters of the bolts were 10 mm and 12 mm.

2.2. Beam Specimens. All specimens had the same cross-sectional dimensions, longitudinal reinforcement ratio, and stirrup ratio. Figure 1 presents the dimensions and reinforcement of the RC beams. The beams were 150 mm wide, 300 mm height, and 1800 mm long. Shear span (a) was 700 mm, and the effective depth (d) was 250 mm. Two 25 mm diameter deformed bars were used as the main longitudinal reinforcement, and two 6 mm diameter round bars were used as the compressive reinforcement. The shear reinforcements were also 6 mm diameter round bars. All beams were designed to fail in shear. The stirrup spacing in the tested span (i.e. the left shear span in Figure 1) was 350 mm corresponding to the stirrups ratio of 0.12%. In order to control the side of failure, more stirrups were provided in the right shear span with the spacing of transverse steel of 100 mm and the stirrups amount of 0.38%, as illustrated in Figure 1.

The SFRC panels were used as external shear reinforcements. The panel dimensions were $300 \times 700 \times 10\,\text{mm}^3$. Four SFRC panels were attached to shear span of the RC beams by using epoxy adhesive (i.e. two panels per side as shown in Figure 2). Figure 3 presents the details of strengthening panels. The bolt arrangements differed depending on the number of bolts per panel.

Table 1: Experimental cases.

Beam name	Designation	Connection types	Fiber volume fraction (%)	Number of bolts	Diameter (mm)
Control beam	RC beam	—	—	—	—
1.5F-Epoxy	Strengthened	Epoxy	1.5	—	—
0F-8D12	Strengthened	Epoxy + bolts	0.0	8	12
1F-8D12	Strengthened	Epoxy + bolts	1.0	8	12
1.5F-8D12	Strengthened	Epoxy + bolts	1.5	8	12
1.5F-4D12	Strengthened	Epoxy + bolts	1.5	4	12
1.5F-6D12	Strengthened	Epoxy + bolts	1.5	6	12
1.5F-6D10	Strengthened	Epoxy + bolts	1.5	6	10
1.5F-8D10	Strengthened	Epoxy + bolts	1.5	8	10

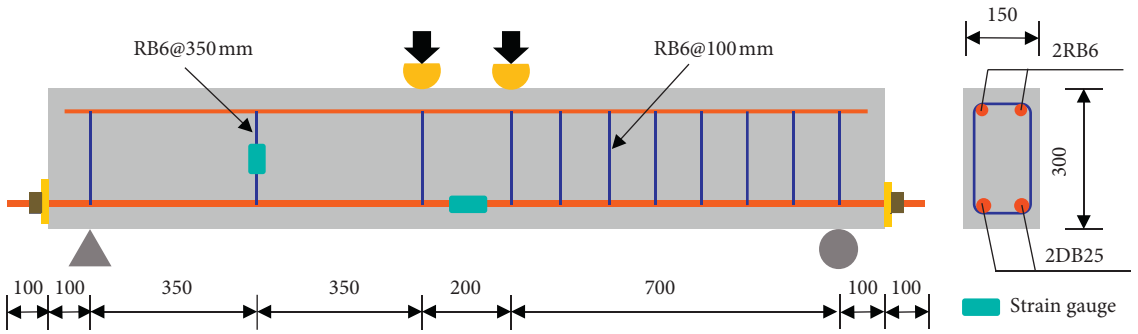

Figure 1: Geometry and reinforcement of RC beams (unit: mm).

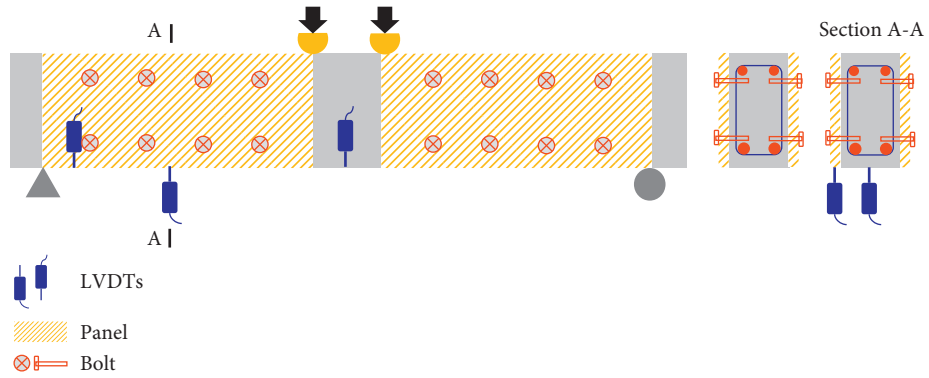

Figure 2: Details of the strengthened specimens and measurements (unit: mm).

2.3. Properties of Materials. Concrete with a design cylinder compressive strength of 30 MPa was used for all beams. The mix proportion of concrete is presented in Table 2. The yield stress of stirrups and tensile reinforcing steel bars were 235 MPa and 502 MPa, respectively. The elastic modulus of both reinforcements was 200 GPa. For the SFRC panels, the commercially available high-strength mortar (Lanko 701) was mixed with hooked-end steel fibers. The water to binder ratio was 0.175 by weight, as suggested in the product guidelines. Table 3 lists the properties of steel fibers, and the fiber volume fractions were 0%, 1.0%, and 1.5%. In addition, the mechanical properties were ranging 56.8–69.7 MPa and 3.77–5.34 MPa for compressive and tensile strengths, respectively.

The panels were bonded on the beams using a two-component epoxy adhesive (Sikadur-30) with a tensile strength of 29 MPa, shear strength of 18 MPa, and elastic modulus in tension of 11.2 GPa, as given by the manufacturer. In addition, 10 mm and 12 mm diameter chemical bolts (anchoring rod: HIT-V5.8 and injection mortar: HIT-HY 200-R) were used in this study.

2.4. Specimen Preparation. After casting, the RC beams were sprayed by water daily and covered by wet cloth and plastic sheet for 28 days. Strengthening panels were cast of 10 mm thickness, and the locations of bolts on panels were fixed by providing holes on panels in the casting step. The panels were demolded after 24 hours and were cured in water for 7 days. Before strengthening, concrete and panel surfaces were roughened by using a concrete grinder and cleaned by using a air blower to remove dust. Then, the epoxy adhesive was applied on the concrete and panel surfaces. Next, the precast panels were attached to the side of the beams. For the

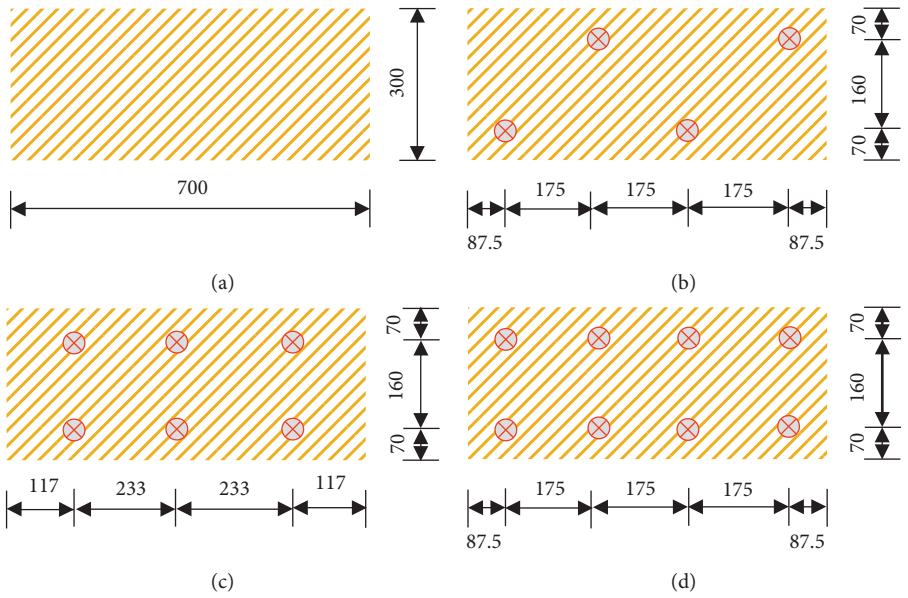

Figure 3: Panel geometry and bolt arrangement (unit: mm). (a) No bolt. (b) 4 bolts. (c) 6 bolts. (d) 8 bolts.

Table 2: Mix proportion of concrete.

Water to binder ratio	Water (kg/m^3)	Cementitious materials (kg/m^3)	Fine aggregate (kg/m^3)	Coarse aggregate (kg/m^3)	Admixture (cc/m^3)	Slump (cm)
0.54	185	342	770	1,150	1,710	12.5

Table 3: Properties of steel fibers.

Type	Length (mm)	Diameter (mm)	Aspect ratio	Tensile strength (MPa)	Elastic modulus (GPa)	Shape of the end
Steel	35	0.55	65	1050	210	Hooked end 

specimens with bolt connections, after attaching the panels, RC beams were drilled to make holes. After cleaning the holes, adhesive was injected and anchoring rods were finally installed.

2.5. Testing and Instrumentation. All beams were tested as simply supported beams under two symmetrical point loads as shown in Figure 2. In order to reflect the actual behavior of the existing structures, the load was applied on loading plates placed on the RC part. It is because in real structures, the RC beams have already carried the load before strengthening. Then, the strengthening panels have been used to improve the load capacity of the existing structures. Therefore, the load was applied on only the existing RC part to investigate the improvement in the load capacity after strengthening. The strain of longitudinal rebar at midspan and strain of stirrup at the middle height were measured using strain gauges. Locations of steel strain gauges are illustrated in Figure 1. Midspan deflection of the RC beams was measured using linear variable displacement transducers (LVDTs) as shown in Figure 2. Additionally, the deflection of the panels was also measured using LVDTs. Herein, two LVDTs were set under specimens to measure the vertical displacements of the RC beam and panel at the middle of the shear span (section A-A) as presented in Figure 2. Furthermore, the displacement control was used with rate of 0.005 mm/s up to the failure of the beams.

3. Experimental Results and Discussion

3.1. Overall Responses

3.1.1. Load-Deflection and Load-Reinforcement Strain Relationships. Load-displacement responses of eight RC beams strengthened with SFRC panels were compared to that of the control beam without strengthening, and the load-deflection curves, referring to the total applied load and the midbeam deflection, are presented in Figures 4 and 5. At the beginning, before flexural cracking occurs, the initial load-deflection response linearly increased with applied

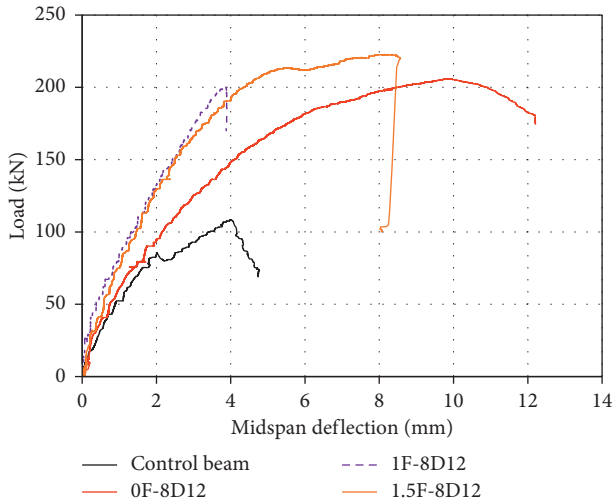

Figure 4: Load-deflection curves for beams with different steel fiber volume fractions.

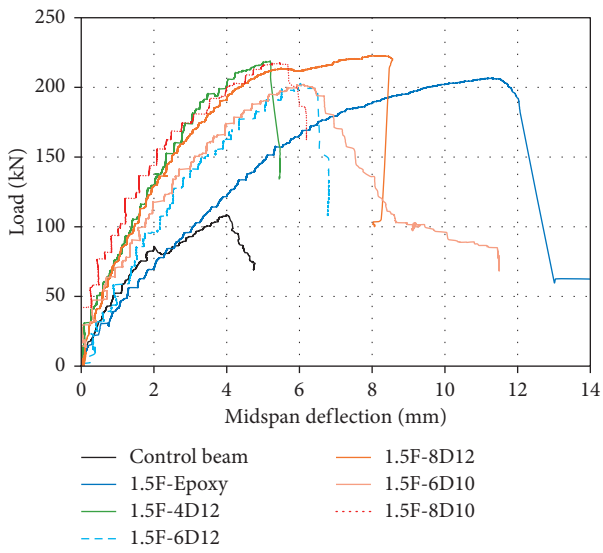

Figure 5: Load-deflection curves for beams with various connection details.

load. Then the stiffness of beams slightly decreased by initiation of flexural cracks at the load level of 30 kN approximately. Diagonal crack was then first observed at the shear span resulting in the abrupt stiffness reduction of the control beam, 80 kN approximately, since the concrete property is the same in all specimens. It is obviously observed in Figures 4 and 5 that abrupt stiffness reduction was not evident in the strengthened beams because the strengthening system maintained the shear resisting mechanism in those beams. Therefore, the load still increased with lower stiffness until reaching the peak load. Stirrups in all beams were yielded at this stage as shown in Figure 6. After that, the load suddenly dropped and shear failure occurred in all beams. As presented in Figures 4 and 5, all strengthened RC beams resisted higher load capacity than those of the control beam. The aforementioned observations imply that the shear performances of the beams

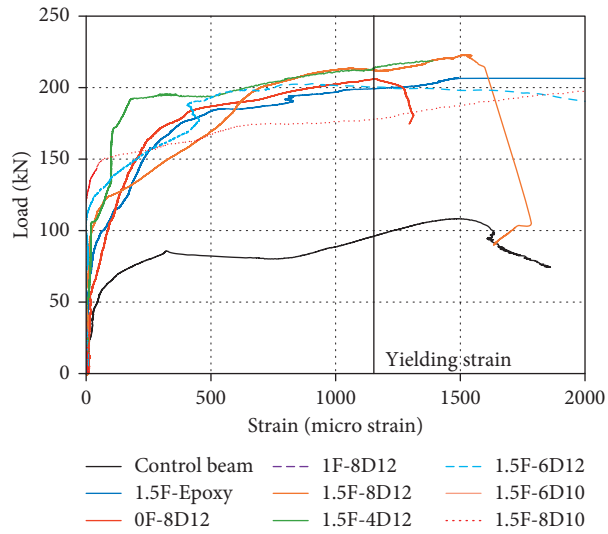

Figure 6: Load versus strain developed in the stirrups.

strengthened in shear with SFRC panels are improved in the load capacity. Moreover, as observed in Figures 4 and 5, the area under the load-deflection curves of the strengthened specimens is significantly greater than the area under the load-displacement curve of the reference beam, indicating the improvement in the ductility of the beams with the SFRC precast systems.

3.1.2. Crack Pattern and Failure Mode. It is obvious from the test that a diagonal crack was clearly visible in the control beam. The diagonal crack was first observed at the middle height of the beam and then propagated to the support and loading point. The control beam failed when the concrete compression zone was crushed so that diagonal tension failure occurred.

To assess the cracking mechanism of the beams strengthened in shear with SFRC panels, Table 4 presents cracking failure formed in the panels at ultimate load of the tested specimens. Additionally, the comparison in the cracking patterns between the test and the simulation is also shown. The simulated cracking is further discussed in the numerical analysis in the following Chapter. As observed from Table 4, in which the epoxy connection (specimen 1.5F-Epoxy) was used for strengthening the beams, no cracks were observed on the SFRC panels from both the test and simulation. However, at the ultimate load, one SFRC panel attached in the specimen 1.5F-Epoxy fell off without warning due to the lack of bonding and a diagonal crack was found on the concrete surface of the original RC beam. In this case, shear failure of the strengthened beam leads the debonding of the SFRC panel. In addition, the stiffness of the specimen 1.5F-Epoxy was less than that of other specimens as seen from its lower slope of the load-deflection curve in Figure 5. Moreover, since no cracks were observed on the SFRC panels, the bridging effect from fibers has not been utilized. The strength of 1.5F-Epoxy is high because the shear resisting force was carried by the RC beams. To improve the

Table 4: Crack pattern of the panels at ultimate load obtained from tests and FE analysis.

Beam	Crack pattern from experiments	Principal strain from FE analysis
1.5F-Epoxy		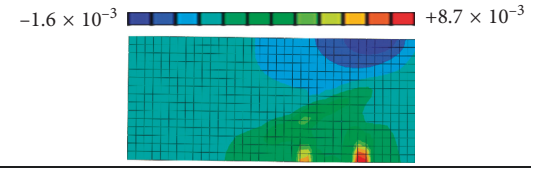
0F-8D12	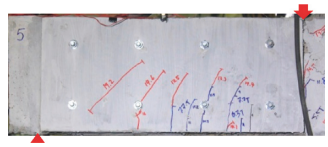	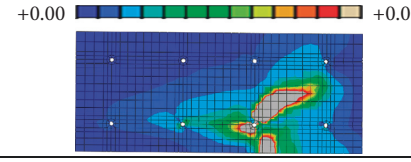
1F-8D12	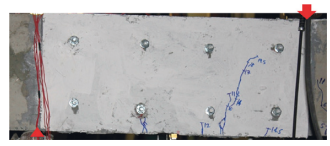	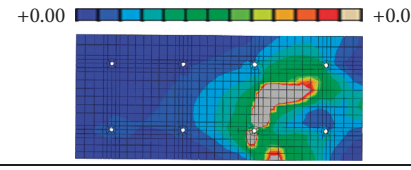
1.5F-8D12	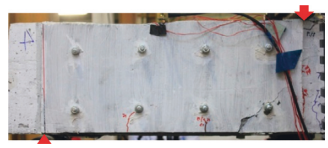	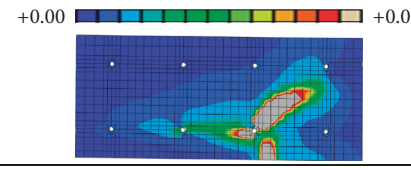
1.5F-4D12		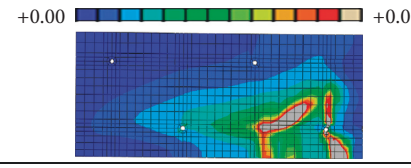
1.5F-6D12		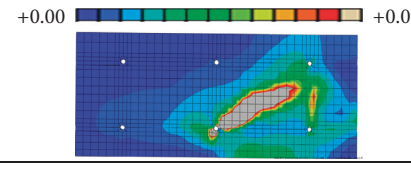
1.5F-6D10	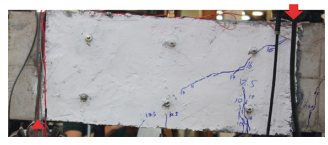	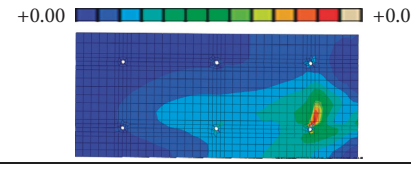
1.5F-8D10	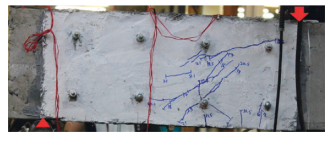	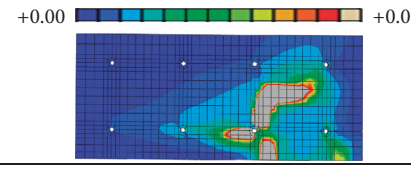

strengthening performance, the additional device should be provided.

On the contrary, the debonding of the panels was not observed in the specimens with SFRC panels attached by using epoxy and bolt connections. In those beams, all panels remained in the beam sides until the test was completed since the bolts together with epoxy adhesive is responsible to hold the panels. Moreover, the local debonding between the bolts or at the free ends was not observed.

A number of cracks were observed in the mortar panels (specimen 0F-8D12) as shown in Table 4. This may mainly be due to the lower tensile strength of the mortar without fibers compared to the other specimens.

Nonetheless, the number of cracks on the strengthened panels with fibers significantly decreased in the comparison with that of the panels with no fibers. Only a few cracks were exhibited in the SFRC panels because the steel fibers make the bridge between the components in the mortar matrix, reducing the internal strain development and cracks. However, also discussed from the studies of Wu et al. [39] and Li et al. [40], the shape of the fibers may affect the crack formation and load capacity of SFRC. Nevertheless, the previous studies [39, 40] clearly reported that the hooked-end shape provided the highest tensile performance comparing with other fiber shapes. When epoxy and bolts were used as connectors, the cracks initially formed near the bolts and normally connected two bolts before penetrating the loading point. This indicates that the location of the bolt in the strengthening system strongly affected the diagonal crack pattern. Furthermore, together with the adhesive, since the bolts were inserted connecting the SFRC panels to the shear span of the beams, the shear transfer mechanism between SFRC and concrete is reasonably activated, utilizing heavily the effectiveness of the strengthening system.

3.2. Shear Strengthening Performance of SFRC Precast Panels under Various Factors. Table 5 reveals the compressive strength of concrete and SFRC, ultimate load capacity (P_{exp}), shear capacity from the experiment (V_{exp}), and shear enhancement ratio, which are derived from the test results. The shear enhancement ratio was calculated as V_{exp} divided by the shear capacity of the control beam. The experimental results show that the shear capacity of the strengthened SFRC beams increased ranging 1.85–2.05 times compared to that of the control beam, implying the strengthening system contributes significantly in the shear carrying capacity. The increase in shear carrying capacity of the strengthened RC beams is due to two reasons as follows: (1) the panels themselves can considerably contribute in shear capacity and (2) the strengthening panels effectively prevents and delays the opening of shear cracks. As seen in Figure 6, at load = 108.4 kN where the peak load of the control beam occurred, the stirrup strains in all strengthened beams were less than that of the control beam. This can confirm that the precast panels can restrain the opening of crack. Hence, the shear resisting mechanism in the strengthened system is drastically triggered, resulting in the enhancement of shear contribution. The effects of various factors, such as steel fiber volume fraction, connection types, number and size of bolts, on the shear effectiveness of the beams retrofitted in shear with SFRC panels are discussed in the following sections.

3.2.1. Effect of Steel Fiber Volume Fraction. Comparison of the shear capacity of four beams with different steel fiber volume fractions is exhibited in Figure 7. Generally, the results show that the shear capacity of RC beams was improved as the strengthening panels were attached and the contents of fiber in panels increased. Actually, the effect of steel fiber volume fraction on shear capacity is not clear by comparing the specimens with SFRC panels having 0% and with 1% of fibers. This means that 1% of steel fibers filled in strengthened panels is not an effective proportion for the use in strengthening the RC beams. However, the shear capacity of the strengthened beams increased as the steel fiber content increased to 1.5%. In fact, the shear carrying capacity of 1.5F-8D12 was 8% and 11% greater than the shear capacities of 0F-8D12 and 1F-8D12, respectively. It is noted that the slight enhancement in the shear capacity can be due to the low thickness of the panels. Moreover, as presented in Figure 4, the increase in steel fiber volume fraction increased the stiffness of the beams since Young's modulus of the steel fiber is great.

Compatibility between the RC beam and panels is also analyzed. Figure 8 presents the relationship between load and vertical displacement of RC beam and panel measured at section A-A and displayed in Figure 2. With regard to the compatibility, vertical displacement between the RC beam and the panel differed from the early stages when mortar panels were used as shown in Figure 8(a). However, with the increase in steel fiber volume fraction, the vertical displacements of the beam and panel became closer as presented in Figures 8(b) and 8(c). This may come from the reduction of a number of cracks in the panels of which steel fibers were added leading to the decrease in the slip between the panels and concrete. Briefly, the increase in steel fiber volume fraction improved shear capacity and stiffness and also decreased relative displacement between panels and beams. The volume fraction of 1.5% of steel fibers is recommended for the practical use to achieve the great shear strength and stiffness.

3.2.2. Effects of Connection Types and Number and Diameter of Bolts. The effect of connection types is presented in Figure 9. In general, the shear capacity of 1.5F-Epoxy is comparable with the beams with epoxy and bolt connections. However, the failure mode of the specimen with epoxy connection is unsafe because 1.5F-Epoxy exhibited suddenly leaving of the SFRC panel to the beam at the peak load. In the specimens installed epoxy-bolt connection, the stiffness (as shown in Figure 5) is significantly improved and the compatibility between the RC part and panel (by comparing Figure 10(a) with Figure 8(c)) is also effective. From the above discussions, it can be pointed out that bolts help shear force to get transfer to the panels and also prevent the debonding of the panels.

Besides, the number of bolts per panel affects the shear capacity of the strengthened beams. The shear enhancement ratio decreased from 2.05 to 1.87 for 12 mm bolts and from 2.01 to 1.87 for 10 mm bolts as the number of bolts decreased from 8 to 6 bolts per panel. However, the different tendency was found when the number of bolts was reduced to 4 bolts per panel and the bolt arrangement was changed to the diagonal pattern (Figure 3(b)). The shear enhancement ratio of 1.5F-4D12 was larger than those for

Table 5: Comparison between experimental and analytical results.

Beam ID	Concrete	SFRC		Experimental results				Analytical results		
	f'_c (MPa)	f'_c (MPa)	f_t (MPa)	P_{exp} (kN)	V_{exp} (kN)	V_{SFRC} (kN)	Shear enhancement ratio	P_{FEM} (kN)	V_{FEM} (kN)	V_{FEM}/V_{exp}
Control beam	32.4	—	—	108.4	54.2	—	1.00	104.1	52.1	0.96
1.5F-Epoxy	32.4	60.8	5.34	206.6	103.3	49.1	1.91	202.0	101.0	0.98
0F-8D12	32.4	56.8	3.77	206.0	103.0	48.8	1.90	207.4	103.7	1.01
1F-8D12	36.7	69.7	4.98	200.2	100.1	45.9	1.85	204.0	102.0	1.02
1.5F-8D12	32.4	60.8	5.34	222.7	111.4	57.2	2.05	218.1	109.1	0.98
1.5F-4D12	36.7	60.8	5.34	219.0	109.5	55.3	2.02	219.3	109.6	1.00
1.5F-6D12	36.7	60.8	5.34	202.8	101.4	47.2	1.87	204.0	102.0	1.01
1.5F-6D10	36.7	60.8	5.34	202.2	101.1	46.9	1.87	205.7	102.8	1.02
1.5F-8D10	36.7	60.8	5.34	217.8	108.9	54.7	2.01	204.7	102.4	0.94

f'_c is the compressive strength. f_t is the tensile strength. P_{exp} and V_{exp} are the maximum load and shear capacity obtained from the experiment, respectively. V_{SFRC} is the shear contribution of SFRC panels ($V_{SFRC} = V_{exp-}V_{exp}$ of the control beam). The shear enhancement ratio is calculated from V_{exp}/V_{exp} of the control beam. P_{FEM} and V_{FEM} are the maximum load and shear capacity obtained from FE analysis, respectively.

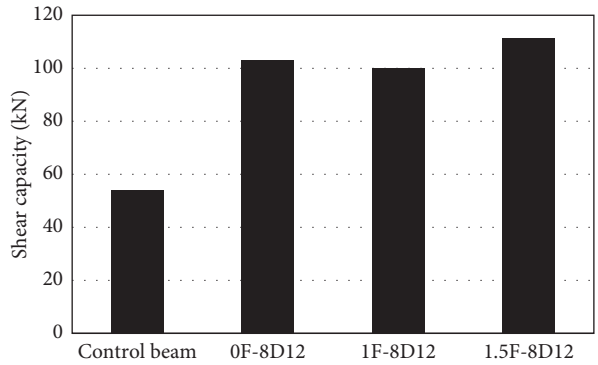

Figure 7: Shear enhancement of beams with different steel fiber volume fractions.

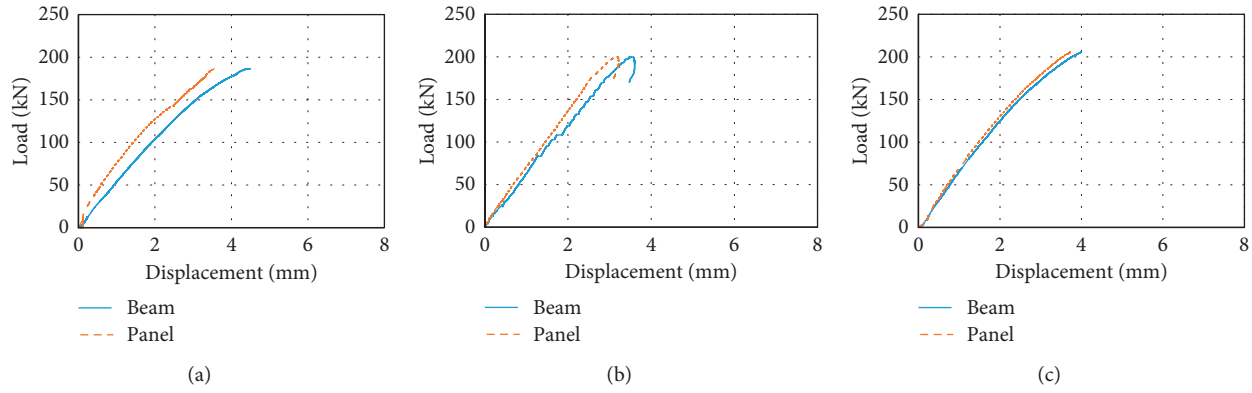

Figure 8: Load versus vertical displacement of the RC beam and panel of specimens with different fiber volume fractions. (a) 0F-8D12. (b) 1F-8D12. (c) 1.5F-8D12.

1.5F-6D12. This implies that the bolt pattern strongly affects the shear capacity of strengthened beams since the bolt arrangement decides the crack propagation in the strengthened beams. The relative vertical displacement between RC beams and panel at the peak load of specimens with epoxy combined with the bolt connection was between 0.21–0.33 mm as presented in Figures 8 and 10. On the contrary, the diameter of the bolts did not much affect the shear strength of the retrofitted beams because the bolts did not fracture. Indeed, the shear capacities of 1.5F-6D10 and 1.5F-8D10 was close to those of 1.5F-6D12 and 1.5F-8D12, respectively. Considering the compatibility, the vertical

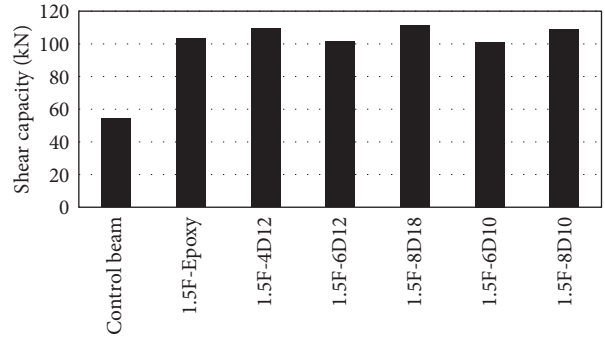

Figure 9: Shear enhancement of beams with various connection details.

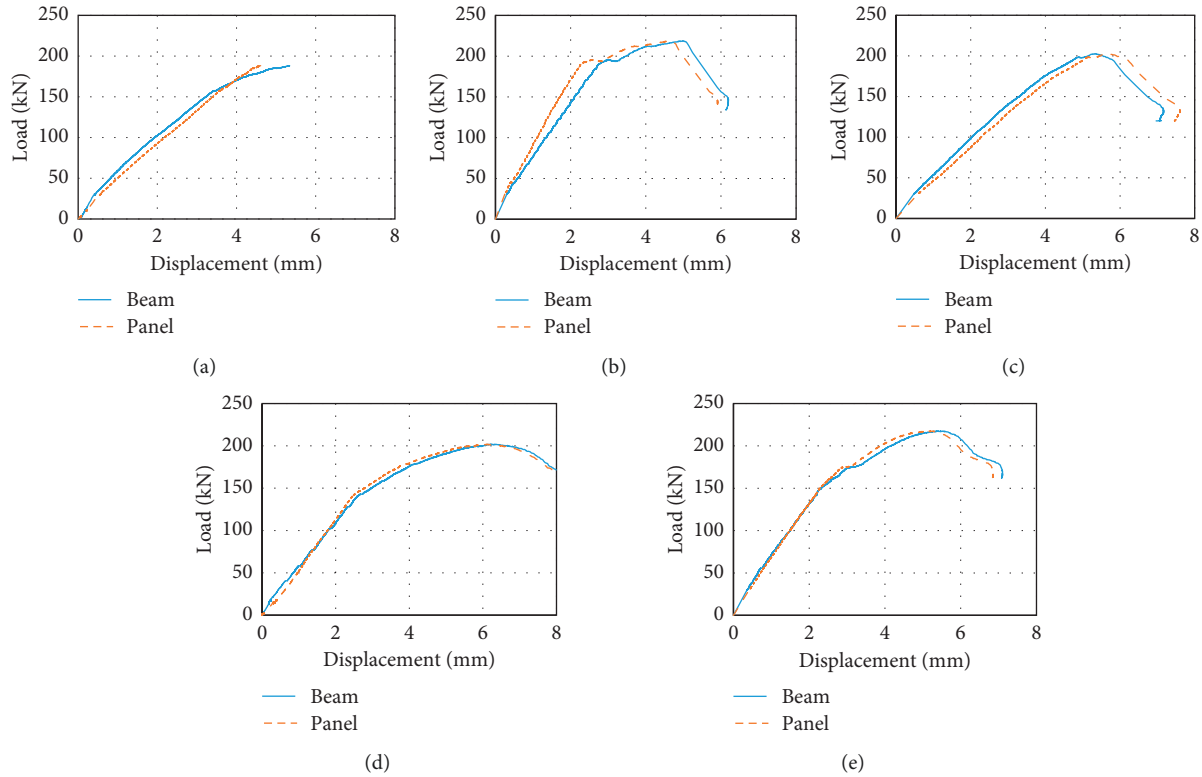

Figure 10: Load versus vertical displacement of the RC beam and SFRC panel with various connection details. (a) 1.5F-Epoxy. (b) 1.5F-4D12. (c) 1.5F-6D12. (d) 1.5F-6D10. (e) 1.5F-8D10.

displacements of the SFRC panel and RC beams were closer in the specimens where a smaller bolt diameter was used as observed in the beams 1.5F-6D10 (Figure 10(d)) and 1.5F-8D10 (Figure 10(e)). Therefore, the bolts with a diameter of 10 mm should be employed in the beams strengthened in shear with SFRC panels through bonding by using adhesive and connecting by using steel bolts.

3.3. Evaluation of Current Shear Prediction Model for Beams Strengthened by Using SFRC Panels. To calculate the shear contribution of SFRC panels (V_{SFRC}), the following equations proposed by JSCE [38] are used in this study:

$$V_{SFRC} = V_{rpc} + V_f, \tag{1}$$

$$V_{rpc} = 0.18\sqrt{f'_{c,SFRC}}\, b_w d, \tag{2}$$

$$V_f = f_v b_w z \cot(\theta), \tag{3}$$

where V_{rpc} (kN) is the shear carried by the matrix of SFRC panels, V_f (kN) is the shear carried by the fibers in the SFRC material, $f'_{c,SFRC}$ (MPa) is the compressive strength of SFRC, b_w (mm) is the web thickness of SFRC, d (mm) is the effective depth (in this study, d equals to the height of the beam since the height of beams was fully covered by panels),

z (mm) is the moment lever arm length ($z = 7d/8$), θ (degree) is the diagonal crack angle what was determined in the cracking pattern of the beams under the failure load, and f_v (MPa) is the average tensile strength perpendicular to the diagonal crack of SFRC. For the calculation, the values of f_v are the same as the tensile strength which are 3.77 MPa, 4.98 MPa, and 5.34 MPa for the fiber volumes of 0%, 1%, and 1.5%, respectively.

Based on the equations above, the calculation of shear contribution of SFRC panels in the seven beams excluding the control beam and the beam 1.5F-Epoxy is carried out. Figure 11 presents the comparison in the shear contribution of SFRC panels between experiment and calculation. As calculated from Figure 11, the mean of the ratio of the calculated shear contribution to the experimental shear resistance of SFRC panels is 0.85 and the coefficient of variation of the mean is 32.7%, showing the acceptable agreement of the shear model of SFRC panels derived by JSCE [38]. Generally, the results computed by the existing model underestimated the actual values except the specimens 1.5F-6D12 and 1.5F-6D10. The reason of the underestimation may be because the influences of connecting system (adhesive and bolts) were not considered in the calculation of the shear contribution of SFRC panels. In addition, substituting the value of f_v by the tensile strength in this calculation also causes to the not good estimation. Even though the JSCE equations [38] are originally applicable for 2% of steel fiber volume, Figure 11 indicates that the amount of 1.5% of steel fiber fraction resulted in the good comparison between experiment and computation since the shear contribution of fibers with high percentage of fiber improves reaching their tensile strength. Due to the sporadic separation of the connecting bolts, changing the crack propagation, and the low fiber content, the specimens 0F-8D12 and 1F-8D12 exhibit the bigger diagonal crack angles, leading to the significant underestimation of the calculation. Besides, the specimens with six connecting bolts results in the easier of cracking mechanism through the bigger spacing of bolts, leading to the small diagonal crack angles. Therefore, the calculated shear contributions of the SFRC panels in these beams are higher than those of the experimental values.

In conclusion, since the JSCE equations [38] were not originally proposed for shear contribution of SFRC-strengthened panels which were linked to the beams' sides by using epoxy and bolts, some influence parameters affecting the shear resisting mechanisms of strengthened RC beams were not included. Hence, the model improvement for calculating the shear resisting force of the retrofitted SFRC component considering multifarious effects, such as thickness of panels, concrete compressive strength, bonding adhesive presence, number of connecting bolts, diameter of connecting bolts, and bolt arrangement, will be further discussed in the next section.

4. Extensive Investigation by means of Finite Element (FE) Analysis

4.1. Analytical Cases Proposed for considering Various Factors. Finite element (FE) modeling of strengthened RC beams was carried out using the available commercial software package ABAQUS. The tested beams were simulated first to validate the effectiveness of the FE tool. Then, FE analysis was performed to investigate the response of the strengthened beams under various effects as a parametric study. Table 6 lists the details of the beams for the parametric study. The effects of panel thickness (series I), compressive strength of SFRC (series II), number of bolts, and bolt pattern (series III) were also considered in the numerical study. The geometry and bolt arrangement of specimens in series I and II are the same as those of 1.5F-8D12. The bolt patterns of the specimens in series III are illustrated in Figure 12.

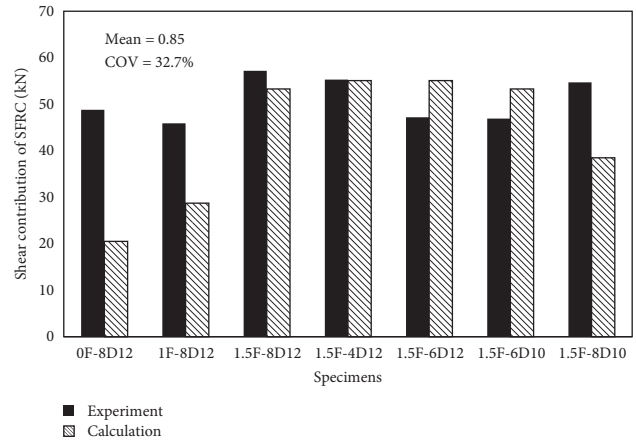

Figure 11: Comparison in shear contribution of SFRC panels between experiment and calculation.

4.2. Element Models. A three-dimensional (3D) FE model was developed. Due to the symmetry of the beams, half of the specimens was modeled as shown in Figure 13(a). Concrete and SFRC elements were modeled using an 8-node brick element with reduced integration (C3D8R) and a 2-node truss element (T3D2) was used for steel reinforcement and stirrups. Longitudinal steel bars were embedded in the concrete element at the specified location without considering the bond-slip between the two elements. Bolts were modeled using an 8-node brick element with reduced integration (C3D8R). Cohesive surfaces defined through the contact area were used to model the bond behavior between the concrete and SFRC panels.

A mesh convergence study was carried out to examine the optimal mesh size. The results show that further decrease in the mesh size has little effect on the numerical results. Consequently, the mesh sizes of the concrete and panels were 20 mm in general and 5 mm for the region near the bolts as presented in Figure 14.

Figure 13(b) shows the loading and boundary condition of the model. A symmetric boundary condition was applied at the plane representing the continuity of the beam. This includes the restrictions of translation along the longitudinal direction (x-axis) and rotation about the out of plane direction (z-axis). Roller support and loading plates were also modeled. In addition, the FE analysis was carried out with the displacement control method.

Table 6: Summary of experimental and analytical results.

Series	Name	SFRC panels				No. of bolts	P_{FEM} (kN)	V_{FEM} (kN)	Shear enhancement ratio
		Thickness (mm)	f'_c (MPa)	f_t (MPa)	ρ_s (%)				
I	B1	15	70	5.24	1.5	8	222.8	111.4	2.06
	B2	20	70	5.24	1.5	8	227.3	113.6	2.10
II	B3	10	50	4.95	1.5	8	202.8	101.4	1.87
	B4	10	90	6.64	1.5	8	221.4	110.7	2.04
III	B5	10	70	5.24	1.5	4	186.4	93.2	1.72
	B6	10	70	5.24	1.5	10	208.8	104.4	1.93

f'_c is the compressive strength, f_t is the tensile strength, ρ_s is the fiber volume fraction, and P_{FEM} and V_{FEM} are the maximum load and shear capacity obtained from FE analysis, respectively. The shear enhancement ratio is calculated from V_{FEM}/V_{exp} of the control beam.

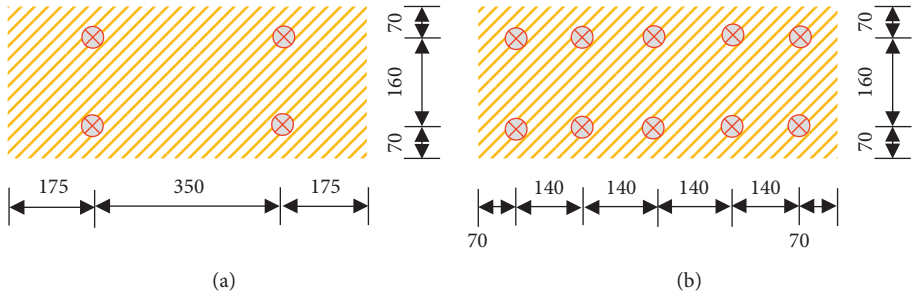

Figure 12: Bolt patterns of specimens in series III (unit: mm). (a) B5. (b) B6.

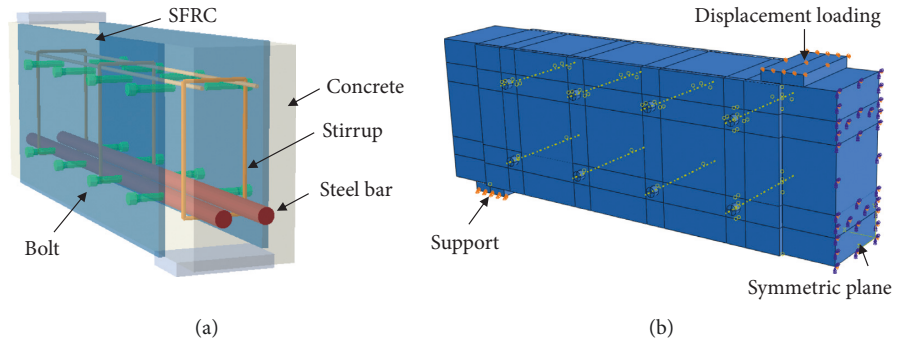

Figure 13: FE model. (a) FE model of 1.5F-8D12. (b) Loading and boundary condition.

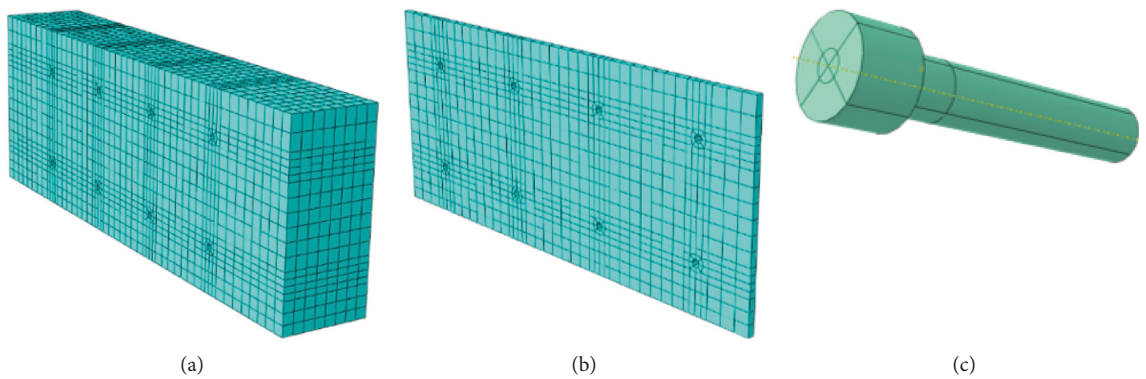

Figure 14: FE mesh discretization. (a) Concrete beam. (b) SFRC panel. (c) Bolts.

4.3. Material Models. In order to model the behavior of concrete, concrete damage plasticity (CDP) was used. The stress-strain curve of concrete in compression was simulated by the model proposed by Hognestad [41]. The tensile behavior was modeled using a linear elastic branch until the tensile strength was reached. After crack initiation, the

fracture energy cracking model was adopted. The fracture energy of plain concrete was calculated from the test results following JCI standard [42] and was equal to 1.79 N/mm.

For the strengthening panels, concrete damage plasticity was also used to simulate the behavior of steel fiber-reinforced concrete. The behavior of SFRC in compression was expressed by the model proposed by Lee et al. [43] as presented in Figure 15(a). The tensile properties of SFRC consisted of the linear elastic behavior until tensile strength was reached and linear softening behavior after crack initiation. The postfailure behavior for direct straining across cracks (Figure 15(b)) was specified by applying a fracture energy cracking criterion, which was calculated from the equations proposed by Kovar and Foglar [44]. Then, fracture energy values are 4.05 N/mm, 7.30 N/mm, and 8.82 N/mm for steel fiber volume fractions by 0%, 1.0%, and 1.5%, respectively.

The longitudinal and shear reinforcements were modeled by a bilinear elastic-perfectly plastic model. The stress-strain behavior of bolts is that of linear elastic material until yielding, followed by plastic behavior. In addition, the modulus of elasticity and yield stress for bolts were taken as 200 GPa and 520 MPa, respectively. On the contrary, as mentioned in the section of element models, a cohesive surface model was used as shown in Figure 16 to define the potential surfaces of separation by traction-separation constitutive model with the values of the bond stress and slip. For the contact between concrete and SFRC, the stiffness coefficient was 4600 N/mm^3 and separation at failure was 0.4 mm. The stiffness coefficient of interface between bolts and concrete/SFRC was 4000 N/mm^3 and separation at failure was 0.06 mm.

4.4. Discussion on Beams' Performances under Various Influences

4.4.1. Validation of FE Model against Test Data. Figure 17 presents an experimental and numerical comparison of the load versus midspan deflection curves of all specimens. As seen from Figure 17, the initial stiffness predicted by FE analysis agreed well with the experimental results in most cases. After the initiation of crack in the specimens, the stiffness of the FE results is slightly higher than that of the experimental results due to the introduction of perfect bond of tension reinforcement to concrete, reducing the displacement in the analyzed beams. In addition, the fact of not considering of concrete shrinkage in the simulation, which results in the less cracking in the beams, may be a reason of the overestimated stiffness. However, the FE modeling can predict well the ultimate load capacity because the beams failed in shear in which the simulation reflected well the actual behaviors. As seen from Table 5, the maximum deviation of analytical shear capacity compared with experimental shear capacity was 6%.

The maximum principal strain at the peak load of the panels obtained from FE analysis is plotted in Table 4 to represent concrete cracking location. It is noted that positive values of strain in Table 4 represent tensile strain and negative values represent compressive strain. Although, it is unable to capture the debonding failure of the specimen due to the limitation of the simulation, as seen in Table 4, the strain contour of 1.5F-Epoxy differs from the strain contour of other specimens because of the debonding of the SFRC panels, which was observed from the test. In other strengthened specimens, it is observed that the diagonal cracks normally pass through the bolts, and clearly this behavior was also observed in this experiment. It is obvious that the failure zone of SFRC panels can be captured from FE analysis. It can be said that the FE modeling is an effective tool in predicting the shear capacity, the cracking patterns, and the failure mode of the RC beams strengthened in shear by using SFRC panels.

4.4.2. Effects of Factors through Parametric Study. The numerical analysis was extended to investigate the effects of panel thickness, the compressive strength of SFRC, the number of bolts, and bolt arrangement on the performances of the strengthened beams. The shear capacity of all analytical beams is listed in Table 5, and the effects of the factors are presented in Figure 18. The results indicate that there was insignificant improvement of shear capacity when the thickness of panels increased from 10 mm to 15 mm and 20 mm (Figure 18(a)). In addition, the shear capacity of the strengthened beams was almost the same as the compressive strength of the SFRC panels exceeding 70 MPa as shown in Figure 18(b). This is because the failure mode may be shifted to the debonding of the panels or the concrete crushing in the compression zone of the beams in the cases of the thicker and higher strength panels.

Figure 18(c) plots the load-deflection curves of the beams with different numbers of bolt per panel. Note that only the specimens with a symmetrical bolt arrangement (B5, 1.5F-6D12, 1.5F-8D12, and B6) are compared in this figure. The results reveal that in the case of the symmetrical bolts pattern, the shear capacity increased as the number of bolts increased from 4 to 8 bolts. This may be because the shear transfer force is reasonably activated in the bolt group. However, the shear capacity decreased as the number of bolts of 10 bolts per panel because providing many bolts per panel reduced the area of the SFRC panels and bolt spacing, which leads the weakness in the shear resisting mechanism. In addition, a crack can easily connect the bolts as the bolt spacing decreased as observed from the strain contour of the specimen with 10 bolts in Figure 19(d). In the case of the smaller number of bolts (4 bolts), since the diagonal arrangement of the connecting bolts may resist the inclined shear crack propagation, the diagonal bolt arrangement (1.5-4D12) exhibited considerably higher shear capacity than that with the symmetrical pattern (B5) as illustrated in Figure 18(d). This finding implies that the bolt arrangement in the SFRC-strengthened beams with the bolt amount less than 4 bolts should be located by using the diagonal pattern.

4.5. Development of Shear Resisting Model for SFRC Panels Connecting by Using Adhesive and Bolts. In the previous

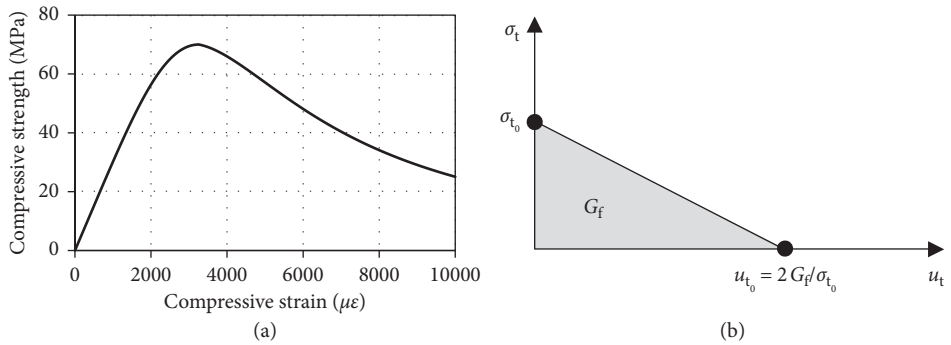

Figure 15: Material model of SFRC. (a) Compression (Lee et al. [43]). (b) Postfailure stress-fracture energy curve.

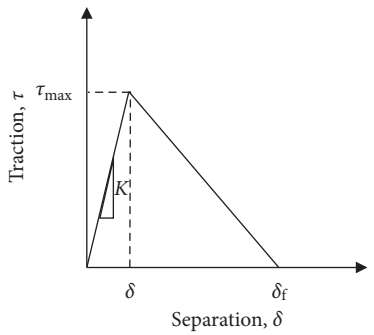

Figure 16: Traction-separation cohesive material law.

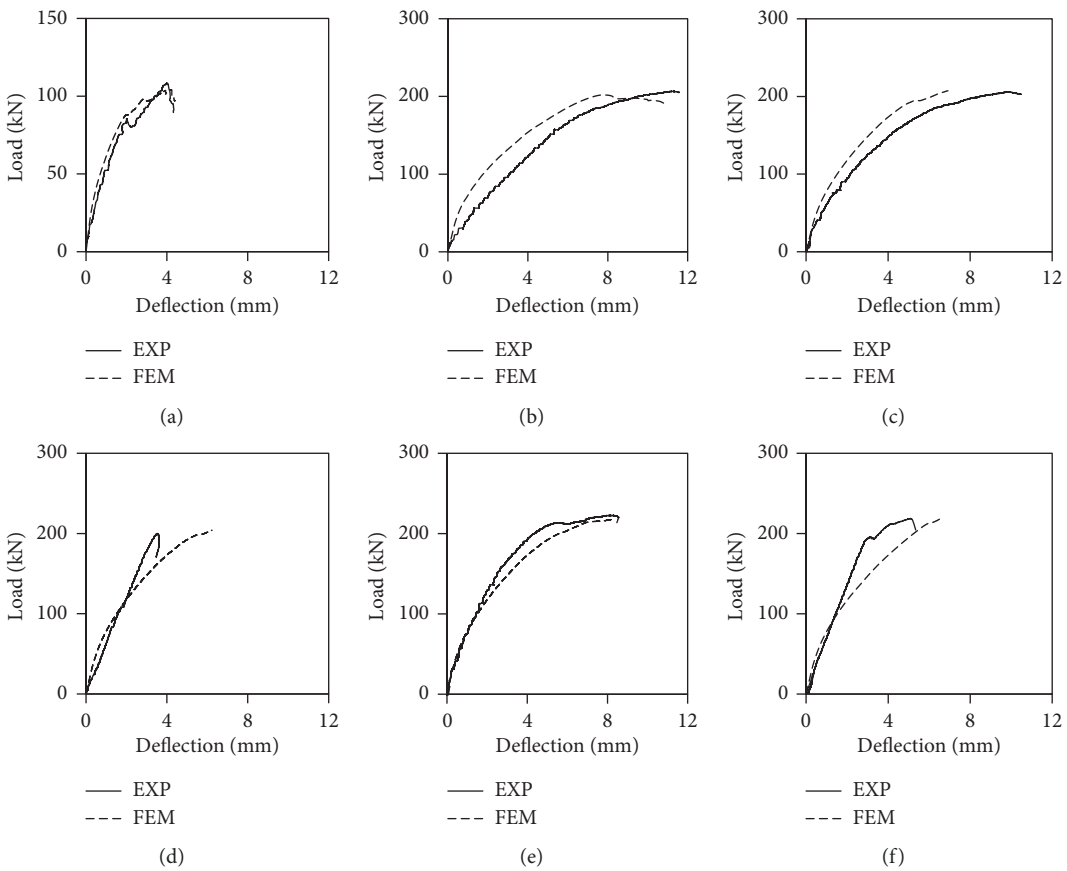

Figure 17: Continued.

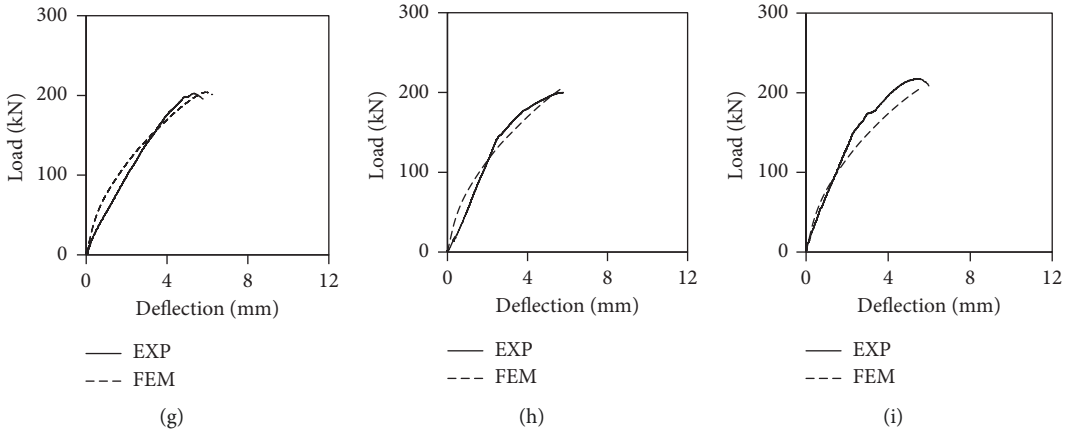

Figure 17: Load-midspan deflection comparison for tested beams. (a) Control beam. (b) 1.5F-Epoxy. (c) 0F-8D12. (d) 1F-8D12. (e) 1.5F-8D12. (f) 1.5F-4D12. (g) 1.5F-6D12. (h) 1.5F-6D10. (i) 1.5F-8D10.

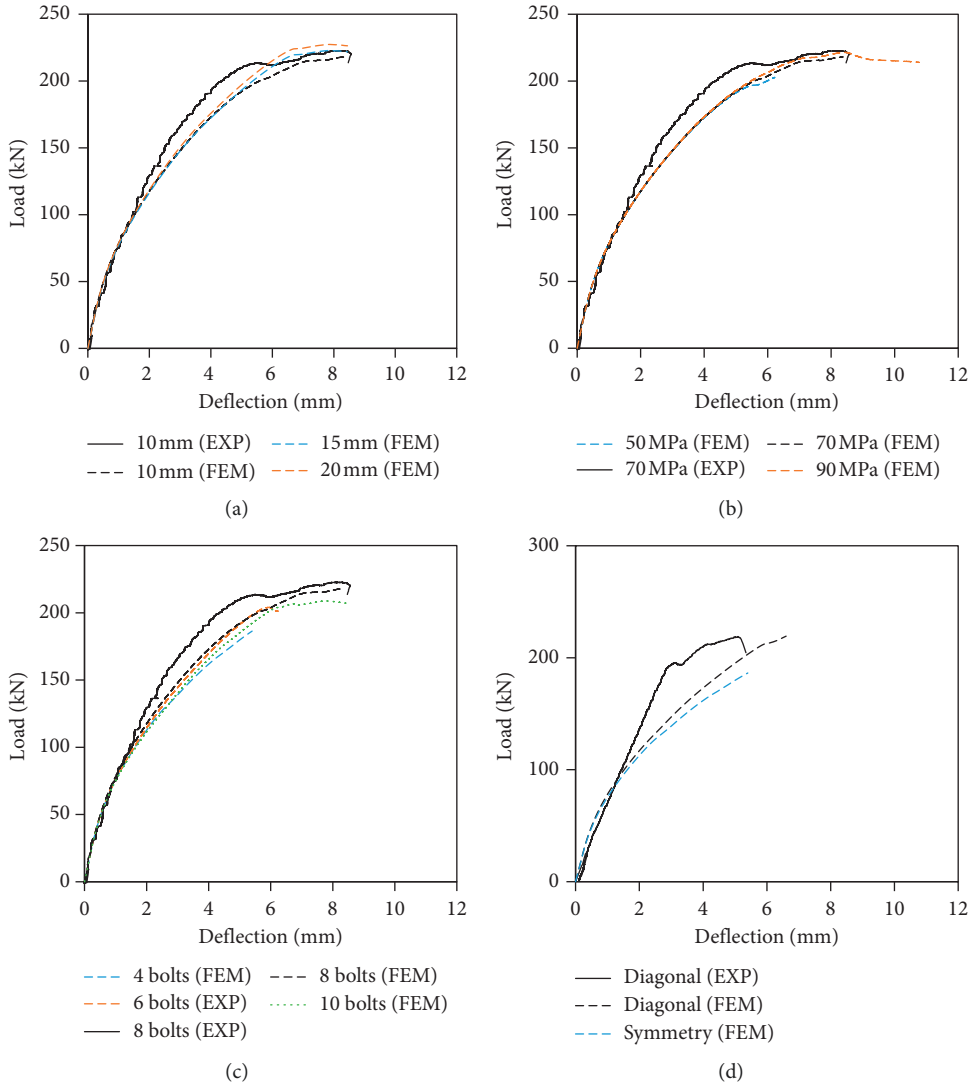

Figure 18: Load-deflection curves of the parametric study. Effect of (a) panel thickness; (b) compressive strength of SFRC; (c) number of bolts (symmetrical pattern); (d) bolt pattern.

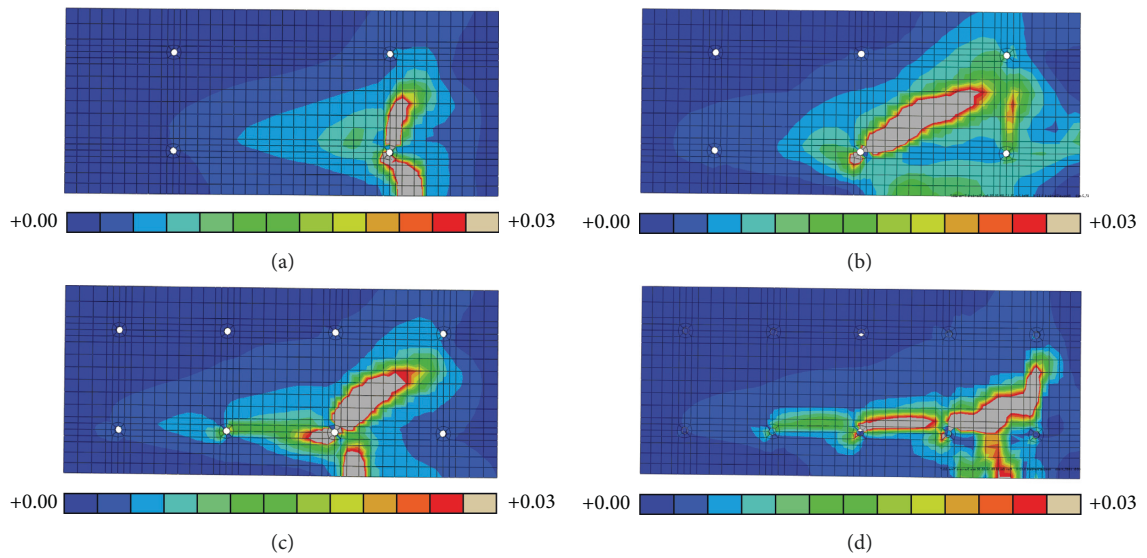

FIGURE 19: Strain at peak load of the panels with different numbers of bolts. (a) 4 bolts (B5). (b) 6 bolts (1.5F-6D12). (c) 8 bolts (1.5F-8D12). (d) 10 bolts (B6).

section, the analysis indicated that the current shear resisting model underestimated the actual values since the connecting bolts are not considered in the calculation. Also, the JSCE equations [38] did not cover in case that the steel fiber volume fractions are less than 2%. In addition, the average tensile strength (f_v) used in the computation by the JSCE formula may not well estimate the actual average tensile strength. In fact, none has ever studied on the formulation of average tensile strength at diagonal crack of SFRC panels taking into account the influences of the connecting bolts, adhesive, and fiber amount. On the contrary, the reliability of the FE simulation has been shown in the sections above. This section, therefore, presents a development of the current model in the shear contribution prediction of SFRC panels connected to the beams' sides by using adhesive and bolts. The shear resisting forces of SFRC panels obtained from the experiment and FE analysis are adopted to propose the new model. Indeed, based on the equations (1), (2), and (3), the average tensile strength perpendicular to the diagonal crack of SFRC (f_v) is calculated and shown in Table 7. It is obvious from Table 7 that the regressing equation for f_v considering all effects, such as stiffness of bolt group and steel fibers, and SFRC compressive strength can be simply built as a three-dimensional linear relationship with R^2 of 0.713 as follows:

$$\frac{f_v}{f_t} = 2.0084 + \frac{1}{(f'_c)^{2/3}}\left(0.0051\frac{nE_bA_b}{A_{panel}} - 0.0093E_s\rho_s\right), \quad (4)$$

where together with the known notations, n is the number of bolts in a group, A_b (mm^2) is the area of bolts, E_b (GPa) is Young's modulus of steel bolts, A_{panel} (mm^2) is the area of the panel, E_s (GPa) is Young's modulus of steel fibers, and ρ_s (%) is the volume fraction of fibers.

By substituting equation (4) into the equations (1)–(3), the shear contribution of SFRC panels is recalculated and against the experimental values. The comparison between the calculation and the investigated values by test and simulation in terms of the shear resisting force of SFRC panels is expressed in Figure 20. The computed results express the good agreement in the prediction of the shear contribution of SFRC panels by employing the proposed equation (equation (4)) for estimating the average tensile strength perpendicular to the diagonal crack (f_v). In fact, the mean value with 1.06 and the coefficient of variation (COV) with 26.7% of the mean of the ratio of the calculated values to the investigated values are exhibited. Of course, obtained results show the better estimation in comparison with the computation achieved from the original model. In addition, the proposed model for predicting the average tensile strength also considers various influences, which much affects the shear resisting mechanism of the SFRC panels in the strengthened beams. In fact, the effects of parameters in equation (4) on the trend of f_v can be well explained complying with the actual behaviors of SFRC. Therefore, the model of JSCE [38] incorporating the proposed equation for f_v could be employed to compute simply the shear contribution of the strengthened SFRC panels inserted to the beams by using bolts and adhesive. Furthermore, the further investigation based on the numerical and experimental study is needed to propose more accurate shear models of the beams strengthened in shear with SFRC panels attached with both bolts and epoxy bonding.

5. Conclusions

This study indicated the importance of the SFRC panels in the shear strengthening effectiveness for the existing RC beams. Based on the experimental and numerical investigations, the following conclusions could be drawn:

(1) Shear capacity of RC beams significantly increased as the RC beams were strengthened using SFRC panels.

(2) The effect of the steel fibers was pronounced when the volume fraction of fiber was 1.5%. The resistance

Table 7: Calculation for the regressing equation of average tensile strength perpendicular to the diagonal crack.

Name	SFRC panels			f_v (MPa)	Stiffness of fiber fraction, $E_s\rho_s$ (GPa)	Stiffness of bolt group, nE_bA_b/A_{panel} (GPa)	f_v/f_t
	Thickness (mm)	f'_c (MPa)	f_t (MPa)				
B1	15	70	5.24	8.30	3.15	0.86	1.58
B2	20	70	5.24	3.72	3.15	0.86	0.71
B3	10	50	4.95	6.90	3.15	0.86	1.39
B4	10	90	6.64	8.59	3.15	0.86	1.29
B5	10	70	5.24	3.67	3.15	0.43	0.70
B6	10	70	5.24	8.53	3.15	1.08	1.63
1.5F-epoxy	10	60.8	5.34	7.74	3.15	0.00	1.45
0F-8D12	10	56.8	3.77	12.39	0	0.86	3.29
1F-8D12	10	69.7	4.98	9.32	2.1	0.86	1.87
1.5F-8D12	10	60.8	5.34	5.81	3.15	0.86	1.09
1.5F-4D12	10	60.8	5.34	5.37	3.15	0.43	1.00
1.5F-6D12	10	60.8	5.34	4.44	3.15	0.65	0.83
1.5F-6D10	10	60.8	5.34	4.58	3.15	0.45	0.86
1.5F-8D10	10	60.8	5.34	8.22	3.15	0.60	1.54

f_v is computed from the experiment and FE based on equations (1)–(3).

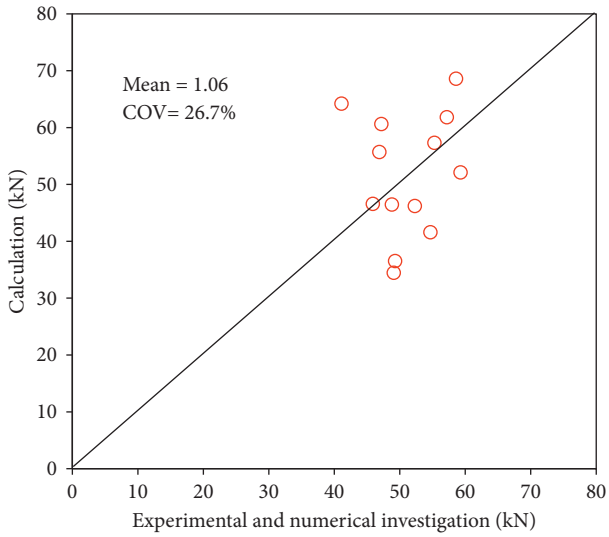

Figure 20: Comparison in shear contribution of SFRC panels between investigation and calculation using the developed model.

to cracks in the panels increased due to the addition of steel fibers. The shear capacity of the specimens with epoxy combined with bolts connection was slightly higher than that with the specimens with only epoxy connection. However, sudden debonding of the SFRC panel was observed at the ultimate load in the case of the specimen with epoxy connection. It is noted that since only one strengthened specimen with the epoxy connection has been tested in this study, further investigation shall be carried out to confirm the behavior of using only epoxy as connection. However, using epoxy combined with bolts connection can prevent debonding and improve stiffness of strengthened beams under service load.

(3) The load-displacement relationships obtained from FE analysis were in close agreement with the experimental results in terms of the ultimate load, crack patterns, and failure mode. This indicates that the presented numerical modeling procedure can be used for predicting the behavior of RC beams strengthened in shear with SFRC precast panels.

(4) The experimental and numerical results showed that the shear capacity increased with the increase in number of bolts up to 8 bolts per panel and compressive strength of SFRC up to 70 MPa. Bolt patterns (also called bolt arrangement) strongly affected the shear behavior of the beams. The diameter of the bolts and panel thickness insignificantly influenced the shear effectiveness of the SFRC strengthened beams.

(5) The shear resisting model of JSCE [38] incorporating the proposed equation (equation (4)) of average tensile strength perpendicular to the diagonal crack (f_v) in this study could predict well the shear resistance of the strengthened SFRC panels installed to the beams by using bolts and epoxy resin under various influences.

(6) For the proposed strengthening method, it is suggested to prepare the panels' holes during casting process. In addition, the drilling of the holes for the bolts on existing RC beams shall be carefully done to avoid the microcraking on the substrate and the possible damage of existing reinforcement. However, some investigations should be conducted in the future such as onsite implementation and the comprehensive evaluation of the current design models.

Data Availability

The data used to support the findings of this study are included within the article. Requests for access of the experimental and analytical data should be made to Dr. Pitcha Jongvivatsakul via email: pitcha.j@chula.ac.th.

Conflicts of Interest

The authors declare that there are no conflicts of interest regarding the publication of this paper.

Acknowledgments

This work was financially supported by the Thailand Research Fund (TRG5880231) and Grants for Development of New Faculty Staff, Ratchadaphiseksomphot Endowment Fund, Chulalongkorn University. The authors would like to acknowledge SR. Fiber Co., Ltd., Hilti (Thailand) Ltd., and Retrofit Structure Specialist Co., Ltd. for providing materials and installation assistance.

References

[1] H. Pham and R. Al-Mahaidi, "Experimental investigation into flexural retrofitting of reinforced concrete bridge beams using FRP composites," *Composite Structures*, vol. 66, no. 1–4, pp. 617–625, 2004.

[2] T. E. Maaddawy and K. Soudki, "Carbon-fiber-reinforced polymer repair to extend service life of corroded reinforced concrete beams," *Journal of Composites for Construction*, vol. 9, no. 2, pp. 187–194, 2005.

[3] A. H. Al-Saidy, A. S. Al-Harthy, K. S. Al-Jabri, M. Abdul-Halim, and N. M. Al-Shidi, "Structural performance of corroded RC beams repaired with CFRP sheets," *Composite Structures*, vol. 92, no. 8, pp. 1931–1938, 2010.

[4] J. M. Sena-Cruz, J. A. O. Barros, M. R. F. Coelho, and L. F. F. T. Silva, "Efficiency of different techniques in flexural strengthening of RC beams under monotonic and fatigue loading," *Construction and Building Materials*, vol. 29, pp. 175–182, 2011.

[5] R. Ghai, P. P. Bansal, and M. Kumar, "Strengthening of RCC beams in shear by using SBR polymer-modified ferrocement jacketing technique," *Advances in Civil Engineering*, vol. 2018, Article ID 4028186, 16 pages, 2018.

[6] G. G. Triantafyllou, T. C. Rousakis, and A. I. Karabinis, "Analytical assessment of the bearing capacity of RC beams with corroded steel bars beyond concrete cover cracking," *Composites Part B: Engineering*, vol. 119, pp. 132–140, 2017.

[7] A. Zhou, R. Qin, L. Feo, R. Penna, and D. Lau, "Investigation on interfacial defect criticality of FRP-bonded concrete beams," *Composite Part B: Engineering*, vol. 113, pp. 80–90, 2017.

[8] M. S. M. Ali, D. J. Oehlers, and R. Seracino, "Vertical shear interaction model between external FRP transverse plates and internal steel stirrups," *Engineering Structures*, vol. 28, no. 3, pp. 381–389, 2006.

[9] C. Pellegrino and M. Vasic, "Assessment of design procedures for the use of externally bonded FRP composites in shear strengthening of reinforced concrete beams," *Composites Part B: Engineering*, vol. 45, no. 1, pp. 727–741, 2013.

[10] T. C. Rousakis, M. E. Saridaki, S. A. Mavrothalassitou, and D. Hui, "Utilization of hybrid approach towards advanced database of concrete beams strengthened in shear with FRPs," *Composites Part B: Engineering*, vol. 85, pp. 315–335, 2016.

[11] M. Vinodkumar and M. Muthukannan, "Structural behaviour of HFRC beams retrofitted for shear using GFRP laminates," *Computers and Concrete*, vol. 19, no. 1, pp. 79–85, 2017.

[12] E. Ferrier, D. Bigaud, J. C. Clément, and P. Hamelin, "Fatigue-loading effect on RC beams strengthened with externally bonded FRP," *Construction and Building Materials*, vol. 25, no. 2, pp. 539–546, 2011.

[13] B. G. Charalambidi, T. C. Rousakis, and A. I. Karabinis, "Fatigue behavior of large-scale reinforced concrete beams strengthened in flexure with fiber-reinforced polymer laminates," *Journal of Composites for Construction*, vol. 20, no. 5, article 04016035, 2016.

[14] J. G. Teng, J. F. Chen, S. T. Smith, and L. Lam, *FRP Strengthened RC Structures*, John Wiley & Sons, Chichester, UK, 2002.

[15] J. F. Chen and J. G. Teng, "Shear capacity of FRP-strengthened RC beams: FRP debonding," *Construction and Building Materials*, vol. 17, no. 1, pp. 27–41, 2003.

[16] C. Diagana, A. Li, B. Gedalia, and Y. Delmas, "Shear strengthening effectiveness with CFF strips," *Engineering Structures*, vol. 25, no. 4, pp. 507–516, 2003.

[17] A. H. Al-Saidy and K. S. Al-Jabri, "Effect of damaged concrete cover on the behavior of corroded concrete beams repaired with CFRP sheets," *Composite Structures*, vol. 93, no. 7, pp. 1775–1786, 2011.

[18] G. G. Triantafyllou, T. C. Rousakis, and A. I. Karabinis, "Corroded RC beams patch repaired and strengthened in flexure with fiber-reinforced polymer laminates," *Composites Part B: Engineering*, vol. 112, pp. 125–136, 2017.

[19] P. Balaguru, R. Narahari, and M. Patel, "Flexural toughness of steel fiber reinforced concrete," *ACI Materials Journal*, vol. 89, no. 6, pp. 541–546, 1992.

[20] V. C. Li, R. Ward, and A. M. Hamaza, "Steel and synthetic fibers as shear reinforcement," *ACI Materials Journal*, vol. 89, no. 5, pp. 499–508, 1992.

[21] F. F. Wafa and S. A. Ashour, "Mechanical properties of high-strength fiber reinforced concrete," *ACI Materials Journal*, vol. 89, no. 5, pp. 449–455, 1992.

[22] P. H. Bischoff, "Tension stiffening and cracking of steel fiber-reinforced concrete," *Journal of Materials in Civil Engineering*, vol. 15, no. 2, pp. 174–182, 2003.

[23] J. Thomas and A. Ramaswamy, "Mechanical properties of steel fiber-reinforced concrete," *Journal of Materials for Civil Engineering*, vol. 19, no. 5, pp. 285–392, 2007.

[24] P. Jongvivatsakul, A. Attachaiyawuth, and W. Pansuk, "A crack-shear slip model of high-strength steel fiber-reinforced concrete based on a push-off test," *Construction and Building Materials*, vol. 126, pp. 924–935, 2016.

[25] A. Meda, S. Mostosi, and P. Riva, "Shear strengthening of reinforced concrete beam with high-performance fiber-reinforced cementitious composite jacketing," *ACI Structural Journal*, vol. 111, no. 5, pp. 1059–1067, 2014.

[26] A. Meda, S. Mostosi, Z. Rinaldi, and P. Riva, "Corroded RC columns repair and strengthening with high performance fiber reinforced concrete jacket," *Materials and Structures*, vol. 49, no. 5, pp. 1967–1978, 2016.

[27] G. Martinola, A. Meda, G. A. Plizzari, and Z. Rinaldi, "Strengthening and repair of RC beams with fiber reinforced concrete," *Cement and Concrete Composites*, vol. 32, no. 9, pp. 731–739, 2010.

[28] K. Kobayashi and K. Rokugo, "Mechanical performance of corroded RC member repaired by HPFRCC patching," *Construction and Building Materials*, vol. 39, pp. 139–147, 2013.

[29] M. Hussein, M. Kunieda, and H. Nakamura, "Strength and ductility of RC beams strengthened with steel-reinforced strain hardening cementitious composites," *Cement and Concrete Composites*, vol. 34, no. 9, pp. 1061–1066, 2012.

[30] V. J. Ferrari, J. B. de Hanai, and R. A. de Souza, "Flexural strengthening of reinforcement concrete beams using high performance fiber reinforcement cement-based composite (HPFRCC) and carbon fiber reinforced polymers (CFRP)," *Construction and Building Materials*, vol. 48, pp. 485–498, 2013.

[31] P. Wirojjanapirom, K. Matsumoto, K. Kono, and J. Niwa, "Experimental study on shear behavior of RC beams using U-shaped UFC permanent formwork with shear keys and bolts," *Journal of Japan Society of Civil Engineers, Ser. E2 (Materials and Concrete Structures)*, vol. 69, no. 1, pp. 67–81, 2013.

[32] G. Ruano, F. Isla, R. I. Pedraza, D. Sfer, and B. Luccioni, "Shear retrofitting of reinforced concrete beams with steel fiber reinforced concrete," *Construction and Building Materials*, vol. 54, pp. 646–658, 2014.

[33] Y. A. Al-Salloum, H. M. Elsanadedy, S. H. Alsayed, and R. A. Iqbal, "Experimental and numerical study for the shear strengthening of reinforced concrete beams using textile-reinforced mortar," *Journal of Composites for Construction*, vol. 16, no. 1, pp. 74–90, 2012.

[34] C. Escrig, L. Gil, E. Bernat-Maso, and F. Puigvert, "Experimental and analytical study of reinforced concrete beams shear strengthened with different types of textile-reinforced mortar," *Construction and Building Materials*, vol. 83, pp. 248–260, 2015.

[35] A. Hemmati, A. Kheyroddin, and M. K. Sharbatdar, "Increasing the flexural capacity of RC beams using partially HPFRCC layers," *Computers and Concrete*, vol. 16, no. 4, pp. 545–568, 2015.

[36] L. Ombres, "Structural performances of reinforced concrete beams strengthened in shear with a cement based fiber composite material," *Composite Structures*, vol. 122, pp. 316–329, 2015.

[37] C. E. Chalioris, G. E. Thermou, and S. J. Pantazopoulou, "Behaviour of rehabilitated RC beams with self-compacting concrete jacketing—analytical model and test results," *Construction and Building Materials*, vol. 55, pp. 257–273, 2014.

[38] Japan Society of Civil Engineers, *Recommendations for Design and Construction of Ultra High Strength Fiber Reinforced Concrete Structures*, JSCE Guidelines for Concrete No. 9, Tokyo, Japan, 2006.

[39] Z. Wu, C. Shi, W. He, and L. Wu, "Effects of steel fiber content and shape on mechanical properties of ultra high performance concrete," *Construction and Building Materials*, vol. 103, pp. 8–14, 2016.

[40] B. Li, L. Xu, Y. Shi, Y. Chi, Q. Liu, and C. Li, "Effects of fiber type, volume fraction and aspect ratio on the flexural and acoustic emission behaviors of steel fiber reinforced concrete," *Construction and Building Materials*, vol. 181, pp. 474–486, 2018.

[41] E. Hognestad, *A Study of Combined Bending and Axial Load in Reinforced Concrete Members*, Engineering Experiment Station, University of Illinois, Urbana, IL, USA, Bullentin Series No. 399, 1951.

[42] Japan Concrete Institute, *Method of Test for Fracture Energy of Concrete by Use of Notched Beams*, JCI Standard, Tokyo, Japan, 2003.

[43] S.-C. Lee, J.-H. Oh, and J.-Y. Cho, "Compressive behavior of fiber-reinforced concrete with end-hooked steel fibers," *Materials*, vol. 8, no. 4, pp. 1442–1458, 2015.

[44] M. Kovar and M. Foglar, "An analytical description of the force-deflection diagram of FRC," *Composites Part B: Engineering*, vol. 69, pp. 550–561, 2015.